Journal of Catalysis **186,** 160–168 (1999)
Article ID jcat.1999.2538, available online at http://www.idealibrary.com on IDEAL®

Carbon Dioxide as Oxidant for the Conversion of Methane to Ethane and Ethylene Using Modified CeO_2 Catalysts

Ye Wang,[1] Yoshimoto Takahashi, and Yasuo Ohtsuka

Research Center for Organic Resources and Materials Chemistry, Institute for Chemical Reaction Science, Tohoku University, Katahira 2-1-1, Aoba-ku, Sendai 980-8577, Japan

Received January 18, 1999; revised April 23, 1999; accepted April 27, 1999

$CaO–CeO_2$ is the most effective catalyst for the conversion at 850°C of CH_4 to C_2H_6 and C_2H_4 by CO_2 among a series of CeO_2 catalysts modified with alkali and alkaline earth metal oxides. When the $CaO–CeO_2$ catalyst is prepared in the range of Ca/Ce ratio 0.1–0.5 by impregnation method, there exist synergistic effects between the two components for the formation of C_2 hydrocarbons, and the catalyst forms solid solution. It is thus suggested that the formation of solid solution is responsible for synergistic effects. The lattice oxygen of the $CaO–CeO_2$ catalyst converts CH_4 mainly to H_2 and CO, and the presence of CO_2 is indispensable for C_2 formation. Both C_2 selectivity and C_2 yield increase remarkably with increasing partial pressure of CO_2, these values at 850°C reaching 75 and 4% at 70 kPa, respectively. Correlation of the results of kinetic analyses and CO_2 TPD measurements indicates that the existence of the pool of the CO_2 chemisorbed on the $CaO–CeO_2$ catalyst accounts for high C_2 selectivity and yield. The characterization of the binary catalyst show that bulk carbonates are not detectable during reaction and Ce^{3+} sites are formed at the outermost layer. It is speculated that these sites activate the chemisorbed CO_2 to generate active oxygen species, which work for the conversion of CH_4 to C_2 hydrocarbons.

Key Words: **methane; carbon dioxide; ethane and ethylene; $CaO–CeO_2$ catalyst.**

INTRODUCTION

Activation and utilization of CH_4 and CO_2, which are both abundant but usually less reactive, are one of the challenging subjects in chemistry. As for CH_4, a large number of papers have been published on its direct conversion, particularly on the oxidative coupling of CH_4 to C_2 hydrocarbons (C_2H_6 and C_2H_4) by O_2 (1–6). The inevitable formation of CO_2, however, seems to be one of the most serious problems from a practical point of view (6). Our novel approach is to use CO_2 as an oxidant instead of O_2. CO will be the only by–product in this case. Moreover, unlike O_2, CO_2 will not induce gas phase radical reactions. In other words, the reaction of CH_4 and CO_2 to produce C_2 hydrocarbons will mainly be controlled by heterogeneous catalyst. It can thus be expected that the development of active catalyst achieves high selectivity to C_2 hydrocarbons.

Equilibrium conversions of CH_4 to C_2H_6 and C_2H_4 in the following reactions are evaluated from thermodynamic calculations (as shown in Fig. 1):

$$2CH_4 + CO_2 \rightarrow C_2H_6 + CO + H_2O \quad [1]$$

$$2CH_4 + 2CO_2 \rightarrow C_2H_4 + 2CO + 2H_2O. \quad [2]$$

The increase in CO_2/CH_4 ratio increases conversions to C_2H_6 and C_2H_4, i.e., yields of C_2H_6 and C_2H_4, which exceed 15 and 25% at ≥800°C for the reactant with CO_2/CH_4 ratio of 2, respectively. These values, if achieved, would meet the target C_2 yield (ca. 30%) estimated from economic evaluations (7). The key point for the realization is to develop an efficient catalyst that is capable not only of activating both CH_4 and CO_2 but also of producing C_2 hydrocarbons selectively.

Only a few studies have been reported on the conversion of CH_4 to C_2 hydrocarbons with CO_2. Enhancement of C_2 formation by CO_2 was observed in the oxidative coupling of CH_4 over a PbO/MgO catalyst (8), but it could not be sustained in the absence of O_2 (9). Our research group has investigated systematically catalytic activities of more than 30 metal oxides for the conversion of CH_4 by CO_2 in the absence of O_2 (10, 11) and found that praseodymium or terbium oxide exhibits relatively good catalytic performance; a C_2 yield of 1.5% with selectivity of ca. 50% is obtained at 850°C (12). A binary oxide of La_2O_3–ZnO was also reported to give a C_2 yield of 2.8% (13). However, such yields are insufficient. Moreover, the role of CO_2 in C_2 formation and the factors controlling the reaction are still unclear.

This work therefore focuses on the development of a more active catalyst system for C_2 formation from CH_4 and CO_2. CeO_2 was selected as a base component of the system, because it showed the highest catalytic activity for the conversion of CH_4 by CO_2 among the metal oxides examined (11). The great redox potential of CeO_2 seems to relate with high CH_4 conversion (>10% at 850°C). However, the

[1] To whom correspondence should be addressed.

0021-9517/99 $30.00

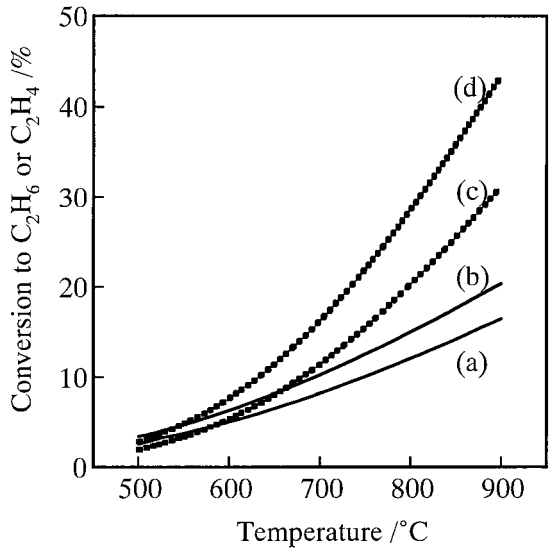

FIG. 1. Equilibrium conversions of CH_4 to C_2H_6 (solid lines) and C_2H_4 (dotted lines) using CO_2 as oxidant. (a) and (c), $CO_2/CH_4 = 1$; (b) and (d), $CO_2/CH_4 = 2$.

major product obtained over CeO_2 alone was CO, and thus C_2 selectivity was negligibly small. It is expected that the modification of CeO_2 with other components may improve C_2 selectivity, and the preliminary study has verified this expectation (14). The present paper clarifies the effect of the modification of CeO_2 with various alkali and alkaline earth metal oxides, in particular the synergistic effect between CaO and CeO_2 in binary catalysts of CaO–CeO_2. The role of CO_2 in the catalysis of C_2 formation and the reaction mechanism are also discussed on the basis of the results of reaction kinetics and chemisorbed species.

EXPERIMENTAL

Catalyst Preparation

Modified CeO_2 catalysts were prepared mainly by impregnating powdery CeO_2 (Rhone–Poulenc, purity >99.5%) with aqueous solutions of alkali and alkaline earth metal nitrates. The surface area of CeO_2 measured by N_2 adsorption was 7 $m^2\,g^{-1}$. The concentration of alkali or alkaline earth metal cation in the solution was 1.0 mol dm^{-3}. The atomic ratio of M/Ce (M = alkali and alkaline earth metal) was 0.2, unless otherwise stated. The impregnation was carried out at room temperature for ca. 12 h. The resultant was calcined at 850°C in an air flow (200 ml min^{-1}) for 4 h after water was evaporated at 90°C. The calcined catalyst was sieved to particles with 16–32 mesh before use. Among these binary catalysts, the CaO–CeO_2 system was mainly used, Ca/Ce ratio usually being 0.5.

A physical mixture of CaO and CeO_2 with Ca/Ce ratio of 0.2 was also used. In this case, CaO, prepared by calcining $Ca(NO_3)_2$ at 850°C in air flow, was thoroughly mixed with CeO_2 for ca. 1 h using an agate mortar.

Catalytic Reaction

The reaction was performed using a conventional fixed-bed quartz reactor operated at atmospheric pressure. The inner diameter of the reactor was 10 mm. For a standard reaction, 2 g of the granular catalyst with size 16–32 mesh was first loaded in the reactor and then calcined again with air (100 ml min^{-1}) at 850°C for 1 h, followed by purge with He (>99.9999%, 100 ml min^{-1}) for 1 h. Finally, a mixture of CH_4 (>99.999%) and CO_2 (>99.995%) was introduced to the reactor. Unless otherwise described, reaction temperature was 850°C, and partial pressures of CH_4 and CO_2, denoted as $P(CH_4)$ and $P(CO_2)$ respectively, were both 30.3 kPa. The total flow rate of the reactants diluted with He was 100 ml min^{-1}.

The effluent gas after removal of H_2O was analyzed by an on-line high-speed gas chromatograph (M200D, Microsensor Technology, Inc.). A MS-5A PLOT column was used for the analysis of H_2, CH_4, and CO. CH_4, CO_2, C_2H_4, and C_2H_6 were simultaneously analyzed with a PORA PLOT-Q column. One analytical run was complete within 150 s, and thus the sampling was repeated every 180 or 300 sec. Data collection was automatically controlled with a computer. The data after 2 h of reaction are described in this paper, unless otherwise stated.

Data processing is based on the assumption that the carbon in CO_2 is converted to CO and the carbon in CH_4 is converted to C_2H_6, C_2H_4, and CO. Thus, CO is produced from both CH_4 and CO_2. The CO from CH_4 is first calculated according to the previous method (10), in which almost all of the reactions involving CH_4 and CO_2 are taken into account. Then, CH_4 conversion and selectivity to C_2 hydrocarbons are calculated using the following equations:

$$\text{CH}_4\text{ conversion} = \frac{2[\text{C}_2\text{H}_6] + 2[\text{C}_2\text{H}_4] + [\text{CO from CH}_4]\ (\text{mol})}{[\text{CH}_4] + 2[\text{C}_2\text{H}_6] + 2[\text{C}_2\text{H}_4] + [\text{CO from CH}_4]\ (\text{mol})} \times 100\ (\%)$$

$$\text{C}_2\text{ selectivity} = \frac{2[\text{C}_2\text{H}_6] + 2[\text{C}_2\text{H}_4]\ (\text{mol})}{2[\text{C}_2\text{H}_6] + 2[\text{C}_2\text{H}_4] + [\text{CO from CH}_4]\ (\text{mol})} \times 100\ (\%).$$

C_2 yield is defined as the product of CH_4 conversion and C_2 selectivity.

Catalyst Characterization

Both fresh and used catalysts were characterized using the following methods. The BET surface areas were measured by N_2 adsorption at 77 K using a volumetric apparatus

(NOVA 1200S, Quanta Chrome). The X-ray diffraction (XRD) analyses were performed with an X-ray diffractometer (XRD 6000, Shimazu) using Cu K_α radiation. The X-ray photoelectron spectroscopy (XPS) measurements were made with an ESCA-750 (Shimazu) spectrometer using Mg K_α radiation. The background pressure in the detector chamber was lower than 3×10^{-6} Pa.

CO_2 TPD Measurements

The CO_2 TPD technique was used for examining the chemisorption of CO_2 on the CaO–CeO_2 catalyst with a Ca/Ce ratio of 0.5. Before TPD measurements, the reaction of CH_4 and CO_2 under the same partial pressure of 30 kPa was carried out at 850°C for 2 h, followed by quenching to 100°C and then replacing feed gas with He at 100°C. The TPD run was then performed at a heating rate of 2.5°C min^{-1} up to 950°C in a stream of either He or CO_2 diluted with He.

RESULTS

Performance of Modified CeO_2 Catalysts

Figure 2 shows the results over CeO_2 catalysts modified with various alkali and alkaline earth metal oxides. In accordance with the previous report (11), CeO_2 alone exhibited high CH_4 conversion but very low C_2 selectivity. The modification of CeO_2 with these additives increased C_2 selectivity and C_2 yield, although CH_4 conversion was decreased in most cases. It is noteworthy that the modification with alkaline earth metal oxides leads to higher C_2 selectivity than that with alkali metal oxides, since this is quite different from the observation in the oxidative coupling of CH_4 by O_2 over modified CeO_2 catalysts (15). Among these binary catalysts examined, CaO–CeO_2 showed the highest C_2 selectivity and yield. The following studies focus on this catalyst system.

Synergistic Effect between CaO and CeO_2 for C_2 Formation

The effect of Ca/Ce ratio on the catalytic performance of CaO–CeO_2 is shown in Table 1. In contrast with the case of CeO_2 alone, CaO alone gave very low CH_4 conversion, which suggests that the activation of CO_2 on this catalyst is rather difficult. When the rate of CH_4 conversion per surface area was compared among CaO–CeO_2 catalysts, it increased with increasing Ca/Ce ratio in the range of 0.1–0.5, but decreased upon further increase. It should be noted that all binary catalysts of CaO–CeO_2 provided higher C_2 selectivity than CaO alone. These observations point out that there exist synergistic effects between CeO_2 and CaO for the conversion of CH_4 into C_2 hydrocarbons by CO_2.

When the catalyst with Ca/Ce ratio of 0.2 was prepared by physical mixing, as shown in Table 1, CH_4 conversion and C_2 selectivity were lower than those obtained for the impregnated catalyst with the same Ca/Ce ratio. The rate of CH_4 conversion or C_2 selectivity for the physically mixed catalyst was nearly equal to the arithmetic mean of those observed for each component. Thus, catalyst preparation by the impregnation method led to synergistic effect.

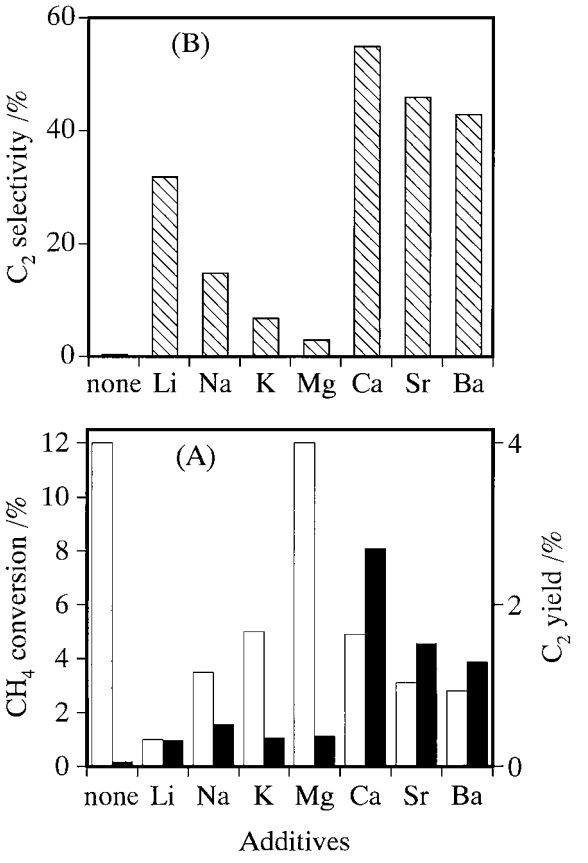

FIG. 2. Effect of the addition of alkali and alkaline earth metal oxides to CeO_2 on the reaction of CH_4 and CO_2. (A) CH_4 conversion (□) and C_2 yield (■); (B) C_2 selectivity. Reaction conditions: $T = 850$°C, $P(CH_4) = P(CO_2) = 30$ kPa.

TABLE 1

Effect of Ca/Ce Ratio on the Performance of CaO–CeO_2 Catalysts

Catalyst[a]	CH_4 conv. (%)	$R(CH_4)$[b] (mmol m^{-2} h^{-1})	Selectivity (%)			C_2 yield (%)
			C_2H_6	C_2H_4	C_2	
CeO_2	12	3.5	0.2	0.3	0.5	0.1
Ca/Ce (0.1)	5.1	3.6	26	20	46	2.3
Ca/Ce (0.2)	4.9	4.0	31	24	55	2.7
Ca/Ce (0.2)[c]	4.0	2.3	6.1	4.0	10	0.4
Ca/Ce (0.5)	5.0	5.2	36	26	62	3.2
Ca/Ce (1.0)	3.4	2.0	28	18	46	1.6
CaO	0.3	0.12	23	13	36	0.1

[a] Atomatic ratio in parentheses.
[b] Rate of CH_4 conversion per surface area.
[c] Prepared by physical mixing of CaO and CeO_2. Reaction conditions: $T = 850$°C; $P(CH_4) = P(CO_2) = 30$ kPa.

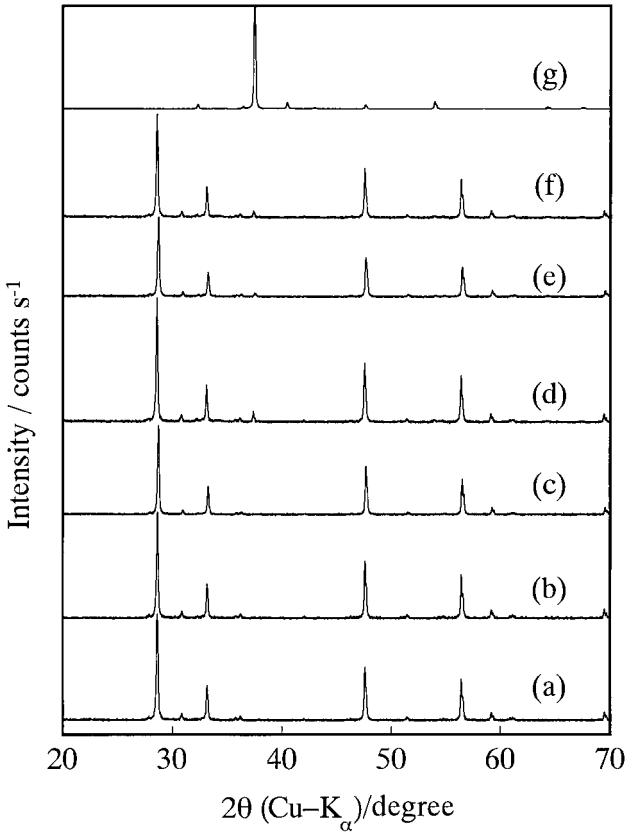

FIG. 3. X-ray diffraction patterns for fresh catalysts. (a) CeO_2; (b) Ca/Ce = 0.1; (c) Ca/Ce = 0.2; (d) Ca/Ce = 0.2 prepared by physical mixing; (e) Ca/Ce = 0.5; (f) Ca/Ce = 1; (g) CaO.

To uncover the nature of such an effect, fresh catalysts were characterized by XRD and XPS. The XRD results are shown in Fig. 3. The diffraction lines observed for CeO_2 alone could be assigned to a typical cubic fluorite structure of CeO_2. Only these lines existed after the addition of CaO to CeO_2 up to a Ca/Ce ratio of 0.2 by the impregnation method, and there were no XRD peaks due to Ca species. When the ratio was increased to $\geq$0.5, the peak of CaO appeared at 2θ(Cu K_α) of 37.5°, but the intensity was very weak. On the other hand, the physically mixed catalyst with a Ca/Ce ratio of 0.2 provided distinct diffraction peaks of CaO that were stronger than those observed for the impregnated sample with a ratio of 1.0. Since CaO can partially dissolve in CeO_2 to form a fluorite-type solid solution (16, 17), the absence of diffraction lines of CaO and the decreased intensities in the impregnated CaO–CeO_2 samples show the formation of solid solution. It is likely that the formation creates a synergistic effect between CaO and CeO_2 in the selective production of C_2 hydrocarbons.

Surface compositions of CaO–CeO_2 catalysts, determined by XPS, are shown in Table 2. Ca/Ce ratios on the surface were always larger than those upon preparation, indicating preferential incorporation of Ca^{2+} into the outermost layer of the CeO_2 matrix. The surface ratio was almost unity when the bulk one was less than 0.5, but it steeply increased upon further increase, which shows the surface coverage by Ca species. This may be the reason for the decrease in both the rate of CH_4 conversion and C_2 selectivity when the Ca/Ce ratio was increased from 0.5 to 1.0, as shown in Table 1. In other words, the cooperation of Ca and Ce components plays a key role in the conversion of CH_4 to C_2 hydrocarbons. The catalyst with a bulk Ca/Ce ratio of 0.5, which exhibited the highest CH_4 conversion rate and C_2 selectivity, is considered in further detail.

Role of CO_2 in the Conversion of CH_4 to C_2 Hydrocarbons

The lattice oxygen of CaO–CeO_2 has been reported to be responsible for the selective formation of C_2 hydrocarbons in the oxidative coupling of CH_4 by O_2 (17). If this is the case in the present study, the role of CO_2 may be the replenishment of the lattice oxygen in place of O_2. To examine this point, the reaction of CH_4 was carried out in the absence of CO_2 over the CaO–CeO_2 catalyst. Although a trace amount of C_2 hydrocarbons was observed, most of CH_4 was converted to H_2 and CO, and the reaction almost stopped after 80 min (14). Therefore, it is unlikely that the lattice oxygen in the CaO–CeO_2 catalyst plays an important role in C_2 formation in the present study.

The change in reaction performance with time on stream in the presence of CO_2 with different partial pressures is shown in Fig. 4. In contrast with the result without CO_2, C_2 hydrocarbons were the main products from CH_4 at higher $P(CO_2)$ of 30 and 70 kPa. Both CH_4 conversion and C_2 selectivity in these cases were almost unchanged during 9–10 h of reaction. When CH_4 conversion was evaluated by two different methods, that is, on the basis of either CH_4 consumed or C_2 hydrocarbons and CO formed (see Experimental), the two values agreed within $\pm$3%, indicating a very good carbon balance. These observations mean there was no significant carbon deposition over the CaO–CeO_2 catalyst. It is thus evident that CO_2 acts as an oxidant for the conversion of CH_4 to C_2 hydrocarbons.

More detailed dependence of the performance of the CaO–CeO_2 catalyst on $P(CO_2)$ is plotted in Fig. 5. CH_4 conversion increased with $P(CO_2)$ but leveled off at $\geq$30 kPa. As $P(CO_2)$ increased, C_2 selectivity increased remarkably and reached 75% at 70 kPa. This finding is noteworthy since

TABLE 2

Bulk and Surface Ratios of Ca/Ce

Ca/Ce used for preparation	Ca/Ce determined by XPS
0.1	0.9
0.2	1.1
0.5	1.3
1.0	3.8

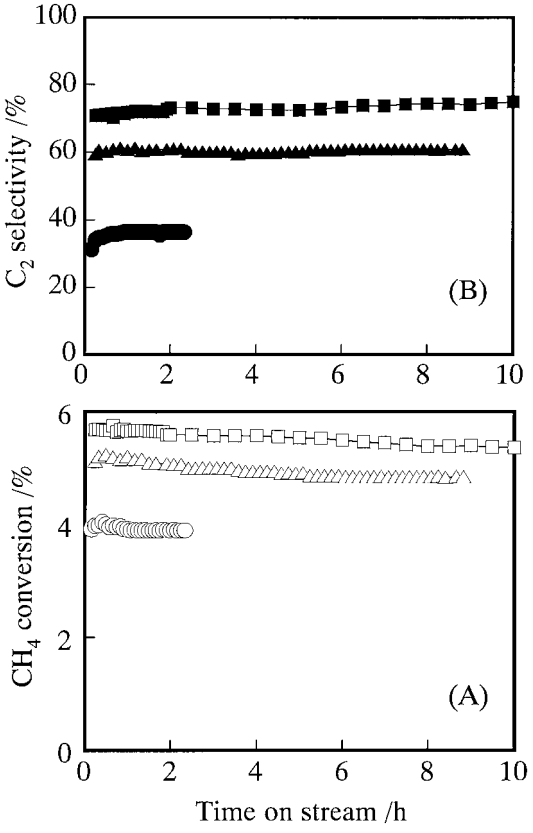

FIG. 4. Reaction performance as a function of time on stream in the presence of CO_2 over the CaO–CeO_2 catalyst (Ca/Ce = 0.5). (A) CH_4 conversion at $P(CO_2)$ of 10 kPa (○), 30 kPa (△), and 70 kPa (□). (B) C_2 selectivity at $P(CO_2)$ of 10 kPa (●), 30 kPa (▲), and 70 kPa (■). Reaction conditions: $T = 850°C$, $P(CH_4) = 30$ kPa.

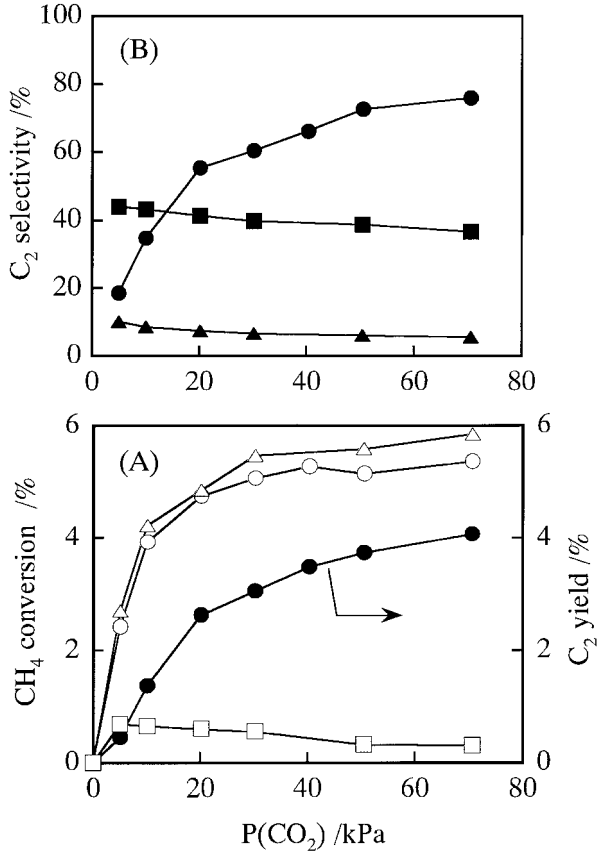

FIG. 5. Dependence of catalytic activity on partial pressure of CO_2 over single and binary oxides. (A) CH_4 conversion over CeO_2 (△), CaO (□), and CaO–CeO_2 (○); C_2 yield over CaO–CeO_2 (●). (B) C_2 selectivity over CeO_2 (▲), CaO (■), and CaO–CeO_2 (●). Reaction conditions: $T = 850°C$, $P(CH_4) = 30$ kPa.

it is usually observed that product selectivity in partial oxidation reactions decreases with increasing partial pressure of oxidant. For comparison, the effect of $P(CO_2)$ over a single oxide of CeO_2 or CaO is also provided in Fig. 5, where 0.5 g of CeO_2 is used in the former case to keep CH_4 conversion at a level similar to that for the CaO–CeO_2 catalyst. C_2 selectivity was much lower over CeO_2 than over the binary catalyst even when compared at the same level of CH_4 conversion. The increase of $P(CO_2)$ did not affect C_2 selectivity over CaO and CeO_2. Almost the same tendency was observed over other modified catalysts, such as MgO–CeO_2, SrO–CeO_2, and BaO–CeO_2. Therefore, the considerable increase in C_2 selectivity with increasing $P(CO_2)$, observed for the CaO–CeO_2 catalyst, is quite unique. These observations point out that CO_2 plays crucial roles in the selective formation of C_2 hydrocarbons over this catalyst.

Kinetic Studies

Further studies were carried out to clarify the nature of the interesting effect of $P(CO_2)$ and to elucidate the reaction mechanism over the CaO–CeO_2 catalyst. Figure 6

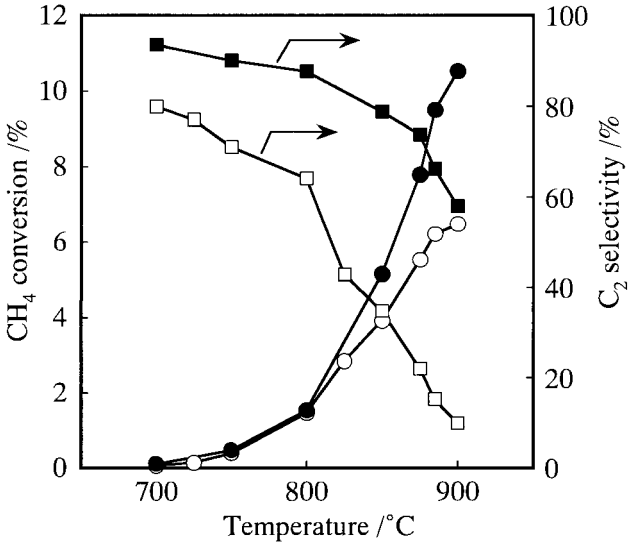

FIG. 6. Dependence of the performance of the CaO–CeO_2 catalyst on reaction temperature. (○) and (●), CH_4 conversion at $P(CO_2)$ of 10 and 70 kPa; (□) and (■), C_2 selectivity at $P(CO_2)$ of 10 and 70 kPa, respectively. Reaction condition: $P(CH_4) = 30$ kPa.

shows the temperature dependence of the catalytic performance at $P(CO_2)$ of 10 and 70 kPa. There was no significant effect of $P(CO_2)$ on CH_4 conversion at temperatures of $\leq$800°C. However, as temperatures exceeded 800°C, CH_4 conversion was higher at higher $P(CO_2)$. Such partial pressure effects became greater at higher temperatures. CH_4 conversion at 900°C was 6.5 and 10.5% at 10 and 70 kPa, respectively.

C_2 selectivity at $\leq$800°C was slightly higher at 70 kPa than at 10 kPa despite the same level of CH_4 conversion. The increase in temperature decreased C_2 selectivity in both cases, but the extent of the decline was more considerable at low $P(CO_2)$ as the temperature was increased to >800°C. As a result, at 900°C, C_2 selectivity at 70 kPa was more than 5 times that at 10 kPa. Although the C_2H_6/C_2H_4 ratio in C_2 hydrocarbons was not shown in Fig. 6, it decreased with temperature, irrespective of the value of $P(CO_2)$. This means that C_2H_6 is the primary product and C_2H_4 is formed by secondary reactions of C_2H_6.

Figure 7 shows the Arrhenius plots for rates of CH_4 conversion at $P(CO_2)$ of 10 and 70 kPa. A good straight line was obtained at 70 kPa in the whole range examined (700–900°C), the apparent activation energy being calculated to be 220 kJ mol^{-1}. On the other hand, at $P(CO_2)$ of 10 kPa, two straight lines with different slopes were required to fit the data. The activation energies calculated were 250 kJ mol^{-1} at $\leq$800°C and 140 kJ mol^{-1} at $\geq$800°C. The former one was similar to that at high $P(CO_2)$.

Figure 8 shows the effect of $P(CH_4)$ on the rate of CH_4 conversion, $R(CH_4)$, at $P(CO_2)$ of 10 and 70 kPa and at 780 and 850°C. At high $P(CO_2)$, $R(CH_4)$ increased proportionally to $P(CH_4)$ irrespective of reaction temperature. Whereas, at low $P(CO_2)$, $R(CH_4)$ at 850°C seemed to level

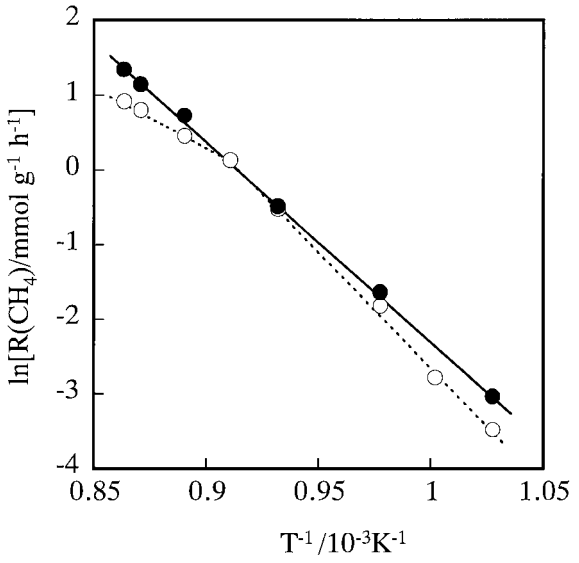

FIG. 7. Arrhenius plots with the CaO–CeO_2 catalyst. (○) $P(CO_2)$ = 10 kPa; (●) $P(CO_2)$ = 70 kPa.

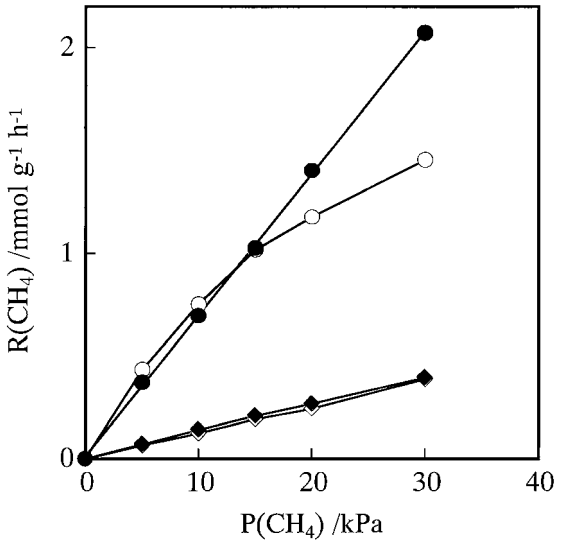

FIG. 8. Dependence of the rate of CH_4 conversion on partial pressure of CH_4. (◇) $P(CO_2)$ = 10 kPa and 780°C; (◆) $P(CO_2)$ = 70 kPa and 780°C; (○) $P(CO_2)$ = 10 kPa and 850°C; (●) $P(CO_2)$ = 70 kPa and 850°C.

off with increasing $P(CH_4)$, viz., the reaction order with respect to CH_4 became less than 1, although $R(CH_4)$ at 780°C increased linearly.

The results described above show that the kinetic features at $P(CO_2)$ of 10 kPa are different from those at $P(CO_2)$ of 70 kPa when the temperature exceeds 800°C.

Chemisorption of CO_2

To examine the chemisorption of CO_2 on the CaO–CeO_2 catalyst after reaction, TPD measurements were carried out. Table 3 shows the TPD results both in He flow and in CO_2 flow with different $P(CO_2)$. Only one desorption peak was observed in every case. The peak temperature was 730°C in He flow. It shifted to 810, 850, and 910°C in CO_2 flow with $P(CO_2)$ of 10, 30, and 70 kPa, respectively. These observations indicate that a pool of chemisorbed CO_2 always exists on the catalyst at temperatures of $\leq$900°C under $P(CO_2)$ of 70 kPa, whereas the pool disappears at >810°C and >850°C under $P(CO_2)$ of 10 and 30 kPa, respectively.

TABLE 3

TPD Results for the Catalysts after Reaction of CH_4 and CO_2 at 850°C

		CO_2 desorption	
Catalyst	$P(CO_2)$ during TPD (kPa)	Peak temperature (°C)	Amount (mmol)
CaO–CeO_2	0	730	0.70
CaO–CeO_2	10	810	0.75
CaO–CeO_2	30	850	0.75
CaO–CeO_2	70	910	0.65
CeO_2	30	No desorption	

As shown in Table 3, the amounts of the CO_2 desorbed were estimated to be 0.65–0.75 mmol, which corresponded to 1/7–1/8 of the amount of CaO in the catalyst. Because no desorption of CO_2 was detectable from CeO_2 alone, Ca species in the CaO–CeO_2 catalyst must account for the chemisorption of CO_2.

Characterization of the CaO–CeO_2 Catalyst after Reaction

The CaO–CeO_2 catalyst after reaction at 850°C under $P(CO_2)$ of 10 or 70 kPa was quenched to room temperature and instantly subjected to XRD analysis. Figure 9 shows that XRD patterns after reaction are independent of $P(CO_2)$ and almost identical to those before reaction. Any diffraction lines of $CaCO_3$ as well as $Ce(CO_3)_2$ or $Ce_2(CO_3)_3$ were not detectable after reaction. Thus, bulk carbonates were not formed during the reaction over the CaO–CeO_2 catalyst. The XRD measurements were also carried out for single oxides of CeO_2 and CaO. Any carbonate phases were not observed for CeO_2 after reactions at both high and low $P(CO_2)$, but CaO was transformed to $CaCO_3$ after the reaction at $P(CO_2)$ of 70 kPa. The absence of $CaCO_3$ in the binary catalyst may indicate that the Ce component plays a role in the activation of the chemisorbed CO_2 during reaction to prevent the formation of bulk carbonate.

Figure 10 shows the Ce 3*d* XPS spectra for the samples before and after reaction under the same conditions as in Fig. 9. According to the Ref. (18), the peaks at 882.3 ± 0.2, 888.6 ± 0.3, 898.1 ± 0.2, 900.2 ± 0.5, 906.2 ± 0.5, and 916.7 ± 0.5 eV can be assigned to v, v'', v''', u, u'', and u''' states of Ce^{4+}, respectively, while the peaks at 885.2 ± 0.3 and 904.0 ± 0.5 eV correspond to v' and u' states of Ce^{3+}. The spectrum before reaction (curve a in Fig. 10) exhibited six peaks ascribed to Ce^{4+}. In addition to them, two shoulder peaks at 885.2 and 903.9 eV clearly appeared after reactions at both high and low $P(CO_2)$, which indicates the existence of Ce^{3+} on the catalyst surface. Moreover, the peaks of Ce^{3+} were stronger at low $P(CO_2)$, suggesting that the concentration of Ce^{3+} on the surface was dependent on $P(CO_2)$. It can thus be speculated that Ce^{3+} sites formed during reaction are responsible for the activation of CO_2.

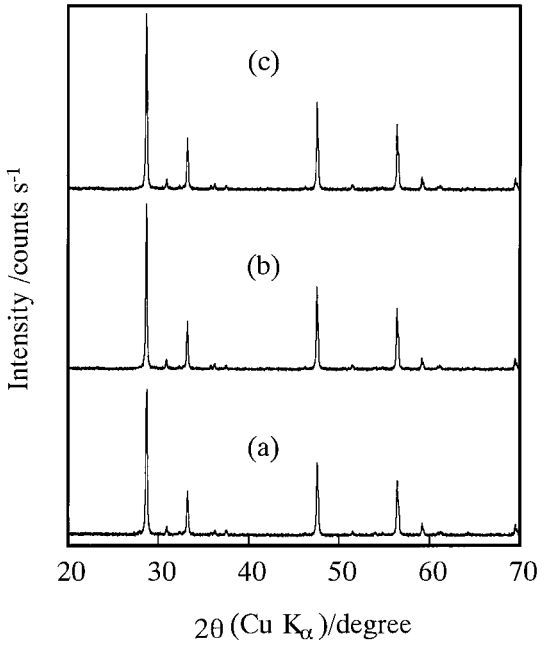

FIG. 9. X-ray diffraction patterns for the CaO–CeO_2 catalyst. (a) Before reaction. (b) and (c) After reaction at 850°C under $P(CO_2)$ of 70 and 10 kPa, respectively.

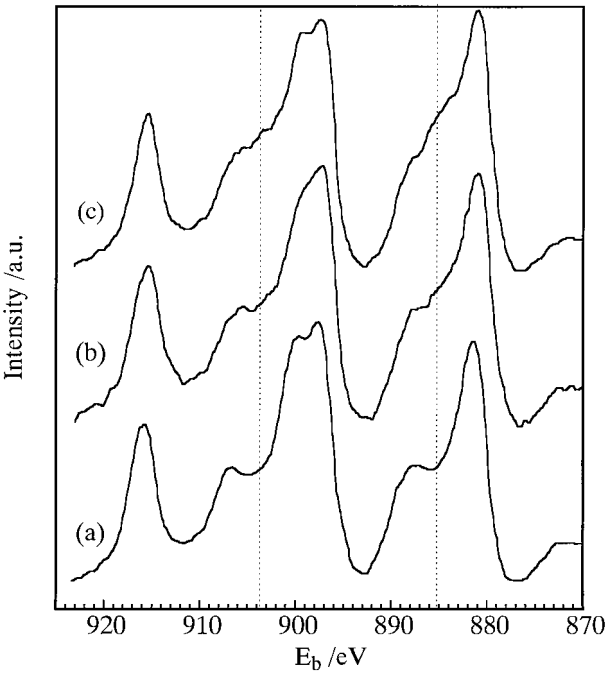

FIG. 10. Ce 3*d* XPS spectra for the CaO–CeO_2 catalyst. (a) Before reaction. (b) and (c) After reaction at 850°C under $P(CO_2)$ of 70 and 10 kPa, respectively.

DISCUSSION

The present work has demonstrated that the modification of CeO_2 with CaO leads to a novel catalyst system effective for the conversion of CH_4 to C_2 hydrocarbons by CO_2 and achieves the highest C_2 yield of 6% at a steady state under the conditions of 900°C and $P(CO_2)$ of 70 kPa. The stable catalytic performance is also noteworthy. Although this yield is still lower than the best one obtained in the oxidative coupling of CH_4 by O_2, the results described here have presented a new route for the simultaneous utilization of CH_4 and CO_2.

Although many papers have been published on CO_2 reforming of CH_4 to produce H_2 and CO using either metal (19) or oxide catalysts (20), high C_2 selectivity observed

over composite catalysts of CaO and CeO_2 shows that such reforming reactions are insignificant under the present conditions and may be suppressed by the CO_2 chemisorbed on the catalysts. The most distinct feature of the present composite catalyst of CaO and CeO_2 is the crucial roles of CO_2 in the formation of C_2 hydrocarbons. The CO_2 TPD of the used catalyst after reaction reveals that a pool of chemisorbed CO_2 exists on the catalyst and the desorption profile depends on $P(CO_2)$ and reaction temperature (Table 3). The combination of these results and catalytic performances at different $P(CO_2)$ and temperatures (Figs. 4–6) shows that the existence of the CO_2 pool leads to high C_2 selectivity. On the other hand, C_2 selectivity dropped after the pool disappeared, for example, at $>810^\circ$C under $P(CO_2)$ of 10 kPa (Fig. 6). The absence of CO_2, that is, the reaction of CH_4 alone, resulted in exclusive formation of CO with trace amounts of C_2 hydrocarbons.

The apparent activation energy for the rate of CH_4 conversion at $P(CO_2)$ of 10 kPa was different below and above 800°C, in other words, higher at $\leq$800°C, whereas that at $P(CO_2)$ of 70 kPa was constant at 700–900°C and similar to the higher activation energy at 10 kPa. Since a pool of the CO_2 chemisorbed on the CaO–CeO_2 catalyst exists both in the whole temperature range under high $P(CO_2)$ and at $<810^\circ$C under low $P(CO_2)$, shown in Table 3, it is probable that the presence of the chemisorbed CO_2 results in higher activation energy.

These observations show different reaction mechanisms before and after desorption of the chemisorbed CO_2. The lattice oxygen of CaO–CeO_2 catalyst may partially be involved when the CO_2 is desorbed. Since C_2 selectivity is low under such conditions, CH_4 may react mainly with the lattice oxygen to form CO and H_2 and the reduced catalyst. The stable performance observed even at low $P(CO_2)$ of 10 kPa (Fig. 4) suggests reoxidation of the oxide by CO_2. As shown in Fig. 8, the reaction order with respect to CH_4 was less than 1 at $P(CO_2)$ of 10 kPa and at 850°C. This may be interpreted as follows; as $P(CH_4)$ increases, the catalyst may be reduced to a larger extent, which results in the decreased concentration of lattice oxygen atoms.

In the presence of the chemisorbed CO_2, on the other hand, the CO_2 pool on the CaO–CeO_2 catalyst may inhibit the reaction via the redox mechanism involving the lattice oxygen and thus lead to high C_2 selectivity. Taking into account the different kinetic features, it is suggested that a different reaction mechanism works for selective C_2 formation. Figure 11 shows the proposed mechanism. Active binary catalysts with Ca/Ce ratios of 0.1–0.5 are present in the form of solid solution (Figs. 3 and 9) and rich in Ca species at the outermost layer (Table 2), which also includes Ce^{3+} sites during reaction (Fig. 10). Thus, CO_2 first adsorbs on the catalyst surface due to interaction with basic Ca^{2+} sites (Fig. 11B), and then the Ce^{3+} sites activate CO_2 to form CO and active oxygen species, possibly O^- (Fig. 11C), which

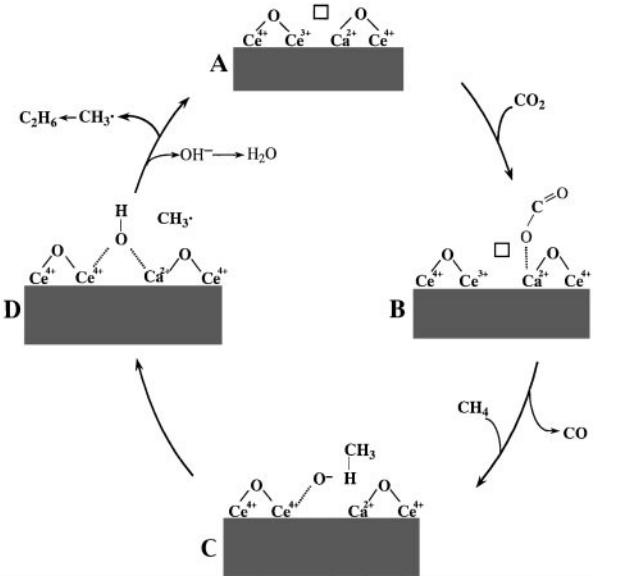

FIG. 11. Proposed mechanism for selective formation of C_2 hydrocarbons over CaO–CeO_2 catalyst.

converts CH_4 to $CH_3\cdot$ radical (Fig. 11D). The involvement of chemisorbed CO_2 in the reaction would lead to higher activation energy than in the case where lattice oxygen participates in activation of CH_4. The formation of solid solution, in other words, the presence of neighboring Ca^{2+} and Ce^{3+} sites, is efficient for CO_2 adsorption and its subsequent activation. Furthermore, the incorporation of bivalent Ca^{2+} cation into CeO_2 lattice generates defect sites, which promote redox reactions between Ce^{4+} and Ce^{3+} (21). This may be the reason for the increase in the rate of CH_4 conversion due to the formation of solid solution between CaO and CeO_2.

CONCLUSIONS

CH_4 is selectively converted to C_2 hydrocarbons by CO_2 using composite CaO–CeO_2 catalysts. The two components in the catalyst show synergistic effects on C_2 formation. The presence of CO_2 is vital for C_2 formation, and C_2 selectivity increases remarkably with increasing $P(CO_2)$. A steady-state C_2 yield of 6% can be achieved with selectivity of ca. 60% at 900°C and $P(CO_2)$ of 70 kPa. The presence of CO_2 chemisorbed on the catalyst surface affects the kinetic features. It is probable that the cooperation of Ca^{2+} and Ce^{3+} sites in solid solution of the catalyst enhances the chemisorption and activation of CO_2 to produce active oxygen species for selective C_2 formation.

ACKNOWLEDGMENTS

This work was supported by a Grant-in-Aid for Scientific Research (B) from the Ministry of Education, Science, Sports and Culture, Japan (No. 10555275).

REFERENCES

1. Pitchai, R., and Klier, K., *Catal. Rev.—Sci. Eng.* **28**, 13 (1986).
2. Lee, J. S., and Oyama, S. T., *Catal. Rev.—Sci. Eng.* **30**, 249 (1988).
3. Hutchings, G. J., Scurrel, M. S., and Woodhouse, J. R., *Chem. Soc. Rev.* **18**, 251 (1989).
4. Krylov, O. V., *Catal. Today* **18**, 209 (1993).
5. Martin, G. A., and Mirodatos, C., *Fuel Process. Technol.* **42**, 179 (1995).
6. Lunsford, J. H., *Angew. Chem. Int. Ed. Engl.* **34**, 970 (1995).
7. Kuo, J. W. C., Kresge, C. T., and Palermo, R. E., *Catal. Today* **4**, 470 (1989).
8. Aika, K., and Nishiyama, T., *J. Chem. Soc. Chem. Commun.* 70 (1988).
9. Nishiyama, T., and Aika, K., *J. Catal.* **122**, 346 (1990).
10. Asami, K., Fujita, T., Kusakabe, K., Nishiyama, Y., and Ohtsuka, Y., *Appl. Catal. A: General* **126**, 245 (1995).
11. Asami, K., Kusakabe, K., Ashi, N., and Ohtsuka, Y., *Stud. Surf. Sci. Catal.* **107**, 279 (1997).
12. Asami, K., Kusakabe, K., Ashi, N., and Ohtsuka, Y., *Appl. Catal. A: General* **156**, 43 (1997).
13. Chen, C., Xu, Y., Li, G., and Guo, X., *Catal. Lett.* **42**, 149 (1996).
14. Wang, Y., Takahashi, Y., and Ohtsuka, Y., *Appl. Catal. A: General* **172**, 203 (1998).
15. Otsuka, K., Shimizu, Y., and Komatsu, T., *Chem. Lett.* 1835 (1987).
16. Arai, H., Kunisaki, T., Shimizu, Y., and Seiyama, T., *Solid State Ionics* **20**, 241 (1986).
17. Zhang, Z.-L., and Baerns, M., *J. Catal.* **135**, 317 (1992).
18. Laachir, A., Perrichon, V., Badri, A., Lamotle, J., Catherine, E., Lavalley, J. C., Fallah, J. E., Hilaire, L., Normand, F. le, Quémére, E., Sauvion, G. N., and Touret, O., *J. Chem. Soc. Faraday Trans.* **87**, 1601 (1991); Normand, F. le, Hilaire, L., Kili, K., Krill, G., and Maire, G., *J. Phys. Chem.* **92**, 2561 (1988).
19. Bradford, M. C. J., and Vannice, M. A., *Catal. Rev. Sci. Eng.* **41**, 1 (1999).
20. Krylov, O. V., Mamedov, A. Kh., and Mirzabekova, S. R., *Catal. Today* **42**, 211 (1998).
21. Trovarelli, A., de Leitenburg, C., and Dolcetti, G., *Chemtech* **27**(6), 32 (1997).